Title
HIGH-TEMPERATURE DEFORMATION MECHANISMS IN SUPERPLASTIC Zn-22A1 EUTECTOID

Author
Vaidya, M.L.

Publication Date
1972-02-01

Submitted to Journal
of Applied Physics

LBL-459
Preprint c.2

HIGH-TEMPERATURE DEFORMATION MECHANISMS IN SUPERPLASTIC Zn-22A1 EUTECTOID

M. L. Vaidya, K. Linga Murty and J. E. Dorn

February 1972

AEC Contract No. W-7405-eng-48

DISCLAIMER

LBL-459

HIGH-TEMPERATURE DEFORMATION MECHANISMS IN SUPERPLASTIC Zn-22Al EUTECTOID

by

M. L. Vaidya*, K. Linga Murty** and J. E. Dorn†
Inorganic Materials Research Division
Lawrence Berkeley Laboratory, University of California
Berkeley, California 94720

ABSTRACT

The temperature and the stress dependences of steady-state strain-rates in Zn-22Al eutectoid were studied by tensile and creep testing using double shear type specimens in a normalized stress (τ/G) range of $\sim 5 \times 10^{-7}$ to $\sim 5 \times 10^{-3}$. The stress dependence of the strain-rate revealed three distinct regions: low stress region (I) with a stress exponent of ~ 1, intermediate stress region (II) with ~ 2 and high stress region (III) with ~ 4. The temperature dependence of the strain-rates in the three regions yielded values of 17.8, 18.9 and 28.8 k Cal/mole for the activation energy for deformation in the regions I, II and III respectively. The value for the activation energy obtained in the regions I and II was identified as that for grain-boundary diffusion while that found in the region III was approximately equal to the self-diffusion value. Whereas strong grain size dependence of the steady-state strain-rates was observed in the regions I and II, the data on all specimens coalesced into a single

*Visiting Scientist. Permanent Address: Department of Metallurgy, Indian Institute of Technology, Kanpur, India

**Research Associate

†Senior Scientist, and Professor of Materials Science, College of Engineering, University of California, Berkeley, California. Deceased September 1971.

line in the region III.

The data revealed d^{-3} and d^{-2} - dependencies of the steady-state strain-rates on the grain size in the regions I and II respectively. The experimental results in the employed stress range obeyed the following phenomenological equation:

$$\frac{\dot{\gamma}kT}{D_b Gb} = A\left(\frac{b}{d}\right)^m \left(\frac{\tau}{G}\right)^n \left(\frac{D}{D_b}\right)^\alpha$$

Here $\dot{\gamma}$ = steady-state shear strain-rate, D_b = grain boundary diffusivity, D = lattice diffusivity, G = shear modulus, b = Burger's vector, d = grain-size, τ = shear stress and A = numerical constant. In the above equation α = o in the regions I and II, and α = 1 in the region III. From the experimental determination of the creep parameters n, m and A, the mechanisms of deformation are identified. Dislocation climb and Coble creep were found to be the controlling mechanisms in the regions III and I respectively. Although the present results in the region II are in close agreement with the predictions based on Ball-Hutchison model for superplasticity, microstructural evidence refutes such a mechanism. The present experimental findings in the whole stress range employed here, however, are in line with the trends predicted in a recent review by Bird, Mukherjee and Dorn.

I. INTRODUCTION

There had been a number of studies on the superplastic behavior of various alloys both from industrial-applicability as well as fundamental viewpoints. Recent reviews[1,2,3] on superplasticity reveal the vast amount of literature available on this subject. Most of the experimental data had been confined to the amounts of neck-free deformation and their relation to the strain-rate sensitivity index, m (= $\partial \ln\sigma / \partial \ln \dot{\varepsilon}$). Systematic studies of the strain-rate dependencies on the stress and the temperature in a wide range are needed to get an understanding into the micromechanics of the deformation characteristics. Recent survey and analyses[4] clearly indicate the lack of experimental data to check the theoretical predictions, especially at extremely low stresses. Even the available data at low stresses are not unambiguous because nonuniform deformation renders the actual stress values doubtful.

Superplasticity is commonly referred to extensive uniform tensile deformation due to rapid increase in the stress with the strain rate. This is analogous to extensive uniform tensile deformation due to rapid increase in the stress with the strain whenever this occurs in high strain-hardening materials at low temperatures, while superplasticity is confined to fine grained ($\sim$1 - 10 μm) materials at elevated temperatures and reasonably low strain rates. Until recently no particular mechanism of deformation is inferred by applying the description 'superplasticity'.[2] However Bird et al[4] categorized superplasticity as a mode of deformation with the steady-state strain-rate being proportional to the square of the stress and inversely to the square of the grain size, and the activation energy for flow being equal to that for the grain boundary

diffusion.[5] From their analyses of the deformation characteristics in terms of the dimensionless parameters, namely $\frac{\dot{\varepsilon}kT}{DGb}$ vs $\frac{\sigma}{G}$ ($\dot{\varepsilon}$: strain rate, D: diffusivity, G: shear modulus, b = Burger's vector, σ: tensile stress and kT has the usual meaning), they could divide the available stress range into 3 parts: (1) high stress region where a dislocation mechanism such as 'dislocation climb' operates,[8] (2) intermediate stresses where 'superplasticity' is observed and (3) low stress range where a stress-directed vacancy diffusion mechanism such as Nabarro-Herring[9-10] or Coble[11] creep contributes predominantly. Thus predicted trends are depicted in Fig. 1.

None of the suggested theories can explain all the currently available data on superplasticity. Avery and Backofen[7] suggested the possibility of Nabarro creep in a Pb-Sn alloy. But strong evidence from recent experimental work refutes the required n = 1 stress dependence. Packer and Sherby[12] analyzed the low stress data of Avery and Backofen using an empirical relationship of the form

$$\dot{\varepsilon} = K \left(\frac{\sigma}{G}\right)^2 \frac{DG}{d^3 kT} , \qquad (1)$$

where K is a constant and d is the grain size, and they obtained an improved agreement. Gifkins and coworkers,[13,14] analyzed their data on Pb-Tl alloys using the semi-theoretical relationship:

$$\dot{\varepsilon} = K' \frac{D_b \sigma}{d^2 kT} , \qquad (2)$$

where D_b is the grain boundary diffusivity. The estimated rates were too slow to account for the experimental data. A studied review of the available data indicates a more satisfactory correlation with σ^2 dependence

in lieu of σ^1 dependence.[4] Such correlations suggest either

$$\frac{\dot{\varepsilon}kT}{DGb} = K\left(\frac{\sigma}{G}\right)^2\left(\frac{b}{d}\right)^2 \quad , \tag{3a}$$

or

$$\frac{\dot{\varepsilon}kT}{D_bGb} = K'\left(\frac{\sigma}{G}\right)^2\left(\frac{b}{d}\right)^2 \quad , \tag{3b}$$

depending on whether the activation energy is that for self-diffusion or grain boundary diffusion. Bird et al's[4] analyses of the data on Zn-Al[5] and Pb-Sn[7] reveal that the constants K and K′ in the above equations differ by four orders of magnitude and also that the latter equation with the grain-boundary diffusivity gives a better correlation. It is to be noted that the equation 3(b) is essentially that given by Ball and Hutchison.[5] The basis for Eq. 3(b) and the underlying assumptions have already been reviewed by Bird et al.[4]

Although a reasonable correlation between theory and experiments is observed at high and moderate stresses (i.e. 'Dislocation Climb' and 'Superplasticity' regions), various inconsistencies were noted at lower stresses. Some of the earlier investigations indicate[6] that dislocation climb may control the deformation at low stresses. However, the data at low stresses indicated strong grain size dependence of the strain rate, an observation inconsistent with a climb mechanism. It is more likely that at these low stresses the deformation mechanism is stress-directed vacancy migration. In a re-evaluation of Ball-Hutchison data[5] on Zn-Al eutectoid as well as Avery-Backofen data[7] on Pb-Sn eutectic, Bird et al[4] proposed that Coble[11] creep may be the dominant mechanism at these extremely small stresses. Unfortunately none of the existing

data extend to low enough stresses to prove their point uneqivocally.

The motivation thus of the present research was to: (1) work with Zn-Al alloy of eutectoid composition; (2) obtain experimental data on steady-state strain-rate as a function of stress in a wide range of stress levels - creep tests for low stress data while Instron tests for high stresses, and achieve high precision in the mechanical data by using double shear specimens thereby avoiding non-uniform deformation; (3) to investigate the grain size dependence of the strain rate; (4) to study the temperature dependence of the deformation rate and determine the activation energies for flow in all the regions covering the available stress range; and finally (5) to correlate the experimental findings with the theoretical expectations and demonstrate the proposed transitions from climb-controlling to superplastic and then to Coble/Nabarro creep regions as lower stresses are encountered.

II. EXPERIMENTAL PROCEDURE

Zn - 22% Al alloy was prepared from 99.999% pure Zn and Al. The alloy was melted in a graphite crucible and chill-cast in a water cooled mold of 1 1/4" dia. The ingots were hot rolled at $\sim$320°C to 7/8" dia. and double-shear specimens of the shape and dimensions as in Fig. 2 were prepared from the rolled stock. The machined specimens were solution treated in an argon atmosphere at 375°C for 15 hours. They were then quenched to ice temperature where spontaneous decomposition produced very fine equiaxed grains of the two phases of the eutectoid. Annealing treatments at 265°C for various times yielded the following grain sizes: (i) 6 hour anneal - $d = 1.19 \pm 0.32$ μm; (ii) 2 days - 2.36 ± 0.26 μm; (iii) 2 weeks - 3.60 ± 0.26 μm; and (iv) 5 weeks - 4.62 ± 0.28 μm. The

grain sizes were determined from the electron micrographs of the surface replicas as the mean linear intercept ($\bar{L}$) and converted to average spatial grain diameter (d) using the relationship $d = 1.75\ \bar{L}$.[5]

The prepared specimens were tested in an Instron testing machine or a suitably designed creep machine at constant load which turns out to be constant stress for the particular configuration of the specimen. An electrically heated oil bath stirred by bubbling argon was used to obtain temperatures above the room temperature. The temperatures were monitored with Chromel-Alumel thermocouples and were maintained constant to $\pm$ 1°. To obtain the low stress data creep tests were conducted and the samples were crept at a constant load (stress) until the steady state was reached and then the load was changed, and again waited until it was clear that the steady state rate was obtained before changing the load again. The length changes were monitored by a Daytronic LVDT and the length measurements were accurate to $\pm\ 5 \times 10^{-5}$ in. The Instron data were obtained by differential strain-rate tests at a constant temperature as described by Vandervoort et al.[15,16] By utilizing the double shear type test specimens uniform elogations and constant steady-state strain-rates were observed to shear strains beyond $\dot{0}.80$[17].

III. EXPERIMENTAL RESULTS

The specimens of the four different grain sizes were tested in a temperature-range from 175-250°C in both an Instron testing machine, and a creep machine for strain-rates smaller than or of the order of 10^{-5} sec^{-1}. Following is an account of the various experimental observations.

(1) Stress Dependence of the Strain-Rate:

Fig. 3 is a double-log plot of the steady-state strain-rate as a

function of the stress at a constant temperature of 250°C. There exist three distinct regions with constant stress exponents. The extension of each region depends on the grain size of the specimen. While there is a strong grain size dependence in regions I and II, the data obtained on all samples merge into a single line at high stresses. Slopes of the lines drawn through the datum points approximate 1, 2 and 4 in regions I, II and III respectively. The values of the stresses at which the transitions occur from regions I to II and II to III depend upon the grain size, and smaller the grain size the higher are the values of these transition-stresses.

Both Instron and creep data were gathered for region II. Only Instron data was taken in region III and only creep data in region I. The differential strain-rate tests in the region III indicated large transients. In the region II these transients were very short, and often the steady states were reached soon after the change in the cross-head speed. The creep curves in the region II revealed either very brief or no primary creep range. In most cases steady-state creep-rates were attained almost immediately upon loading. On the other hand in region I steady-state creep was always preceded by reasonably long transients, the extent of these transient creep regions being dependent on the stress level.

(2) Grain Size Dependence of the Strain-Rate:

It is apparant from Fig. 3 that there is no grain-size dependence of the steady-state strain-rate in the region III. Fig. 4 is a plot of the logarithm of the strain-rate versus the logarithm of the grain size in the regions I and II at stress-levels of 10 and 500 psi respectively

at 250°C. The resulting straight lines indicate d^{-3} - and d^{-2} - dependencies of the strain-rates in the regions I and II respectively.

(3) Temperature Dependence of the Strain Rate:

To determine the activation energies for flow, the temperature dependence of the steady-state creep-rate was studied in all the three regions. Figures 5a, 5b and 5c are plots of '$\ln \dot{\gamma} G^{n-1} T$ vs $1/T$' and the resulting activation energies from the slopes of these straight lines are found to be 17.8 $\pm$ 0.2 k Cal/mole, 18.9 $\pm$ 0.3 k Cal/mole and 28.8 $\pm$ 0.3 k Cal/mole respectively in the regions I, II and III. These values for the activation energy may be compared with that for volume self-diffusion in pure aluminum (33 k Cal/mole)[18] and with those for grain boundary diffusion in zinc (14 k Cal/mole)[19] and in aluminum (16.5 k Cal/mole).* From the recent work of Hassner[20] on the grain-boundary diffusion of Zn in Al-Zn alloys at a constant temperature of 340°C for various concentrations of Zn, a value of 13.2 k Cal/mole is inferred for the activation energy for grain-boundary diffusion in Al-78 Zn if D_o is assumed to be unity.

IV. DISCUSSION

The phenomenological equation applicable for high-temperature diffusion-controlled creep was given by Bird et al[4] to be

$$\frac{\dot{\gamma} k T}{D G B} = A \left(\frac{\tau}{G}\right)^n \quad , \tag{4}$$

where D is the appropriate diffusivity, either volume self-diffusivity or grain-boundary diffusivity. In alloys the appropriate diffusivity

*Assuming that $H_b = \frac{1}{2} H_D$.

is inter or chemical diffusivity

$$D_{alloy} = \frac{D^*_A \, D^*_B}{(N_B D^*_A + N_A D^*_B) f} \quad , \tag{5}$$

where N_A and N_B are the atomic fractions of A and B atoms in a binary AB alloy, D* is the tracer diffusivity and f is the correlation factor. As shown in the earlier section the activation energy for creep in the regions I and II turned out to be near to that for grain-boundary diffusion while that in region III was about 4 k Cal/mole less than that for volume self-diffusion in pure aluminum. The paucity of data in the literature on diffusivities in the alloy makes accurate correlation difficult. To make a master plot of the data covering the entire stress range, Eq. 4 is rewritten as

$$\frac{\dot{\gamma} kT}{D_b G b} = A \left(\frac{\tau}{G}\right)^n \left(\frac{b}{d}\right)^m \left(\frac{D}{D_b}\right)^\alpha \tag{6}$$

where α = o for the regions I and II while α = 1 in the region III. Fig. 6 is a plot of '$\ln \frac{\dot{\gamma} kT}{D_b G_b}$ vs $\ln \frac{\tau}{G}$' and the data obtained on specimens with different grain sizes at various test temperatures (175, 200, 225 and 250°C) are plotted. For simplicity the data obtained in the region III at different temperatures are shown only for a single grain size of 4.6 μm. It is to be noted that the trends observed here are akin to the predictions made by Bird, Mukherjee and Dorn[4] as shown in Fig. 1. To reveal the effect of the temperature on the transition from regions II to III, $\ln \frac{\dot{\gamma} kT}{D_b G b}$ is plotted as a function of $\ln \frac{\tau}{G}$ in Fig. 7 for two different grain sizes (3.6 and 4.6 μm). Included here are also the theoretical trends, expected in region III based on the climb-model, with $A = 6 \times 10^7$, $n = 4$, $m = o$ and $\alpha = 1$ in Eq. 6 above,

applicable for high-temperature creep in pure aluminum[4]. It is assumed that the diffusion frequency factor (D_o) is the same for self-diffusion and grain-boundary diffusion, and $\frac{D}{D_b} = \exp\left(-\frac{H_b}{RT}\right)$. The three different regions depicted in Fig. 6 are analysed in the following.

Region I: This region extends from stresses of the order of $10^{-5}G$ to lower and a strong grain size dependence of the strain-rate is noted. The τ^1 dependence of the creep-rate suggests a diffusion mechanism by vacancy exchange, either Nabarro-Herring[9,10] or Coble[11]. The fact that the activation energy for flow is approximately equal to that for grain-boundary diffusion argues for the Coble mechanism. Further support of the operation of Coble mechanism in this region is obtained through the grain-size dependence of the creep-rate ($\dot{\gamma} \alpha d^{-3}$) as well as the factor A. The experimental value for A was found to be 55 ± 25 compared to 100 predicted by Coble model, while A for Nabarro-Herring mechanism takes a value of 12. It appears from these observations that the Coble mechanism controls the deformation in the region I.

Region II: The analysis of the experimental data in this region indicates that the strain-rate is proportional to $(\frac{\tau}{d})^2$ and the activation energy for deformation may be identified as that for grain-boundary diffusion. These findings are in line with the Ball-Hutchison model[5] for superplastic deformation. As shown in the review paper by Bird et al[4] most of the experimental data available on superplastic creep do correlate with an equation of the form

$$\frac{\dot{\gamma} kT}{D_b G b} = K \left(\frac{\tau}{G}\right)^2 \left(\frac{b}{d}\right)^2 \qquad (7)$$

where K is a numerical constant. The present results yield a value of

302 $\pm$ 216 for K in the above equation. The Ball-Hutchison model predicts a value of $\sim$200 for K. Such an agreement notwithstanding, microstructural observations[21] argue against such a mechanism for superplasticity. Whereas Ball-Hutchison model requires dislocation pile-ups and motion of dislocations through the grain-interior (at least in some grains if not in all), 'marker-experiments' of Nicholson[21] indicate that there is little or no dislocation activity in the grain interior. None of the presently proposed theories explain these experimental observations. In a recent paper Langdon[22] proposed grain-boundary sliding as a deformation mechanism during creep and noted that τ^2 dependence of the creep-rate may be observed at intermediate stresses while τ^1 and τ^4 at low and high stress regions. Although the trends predicted by Langdon[22] are qualitatively identical to the present ones, they however are much different in details. His model for creep due to grain boundary sliding predicts

$$\frac{\dot{\gamma}kT}{DGb} = \beta \left(\frac{b}{d}\right)^1 \left(\frac{\tau}{G}\right)^2 \qquad (8)$$

with $\beta \sim 6$. Whereas this expression yields values of 1 and 2 for m and n respectively, the present results gave 2 and 2 for the same. In addition, Eq. 8 contains the lattice diffusivity while use of the grain boundary diffusivity was necessary to synthesize the present experimental results.

It should be noted that several workers[21,23] believe that the exponent n in Eq. 6 is temperature dependent. If this were true then the activation energy for deformation could not be determined as is done in conventional creep, and here in Figs. 5. As revealed in the

present work n is not a continuous function of the temperature or the stress (except in the transional regions such as between II and III in Fig. 7), but n takes on constant values over certain regions of τ/G, such as those depicted in Fig. 6. Indeed the data presented by Nicholson to show that n is a continuous function of temperature may be replotted in terms of $\frac{\dot{\gamma}kT}{D_b Gb}$ and $\frac{\tau}{G}$ (Fig. 8). It is clear from this analysis that the data at different temperatures merge into a single line with a value of 2 for n while they start deviating at high stresses as conventional creep (climb creep) region is approached (c.f. Fig. 8).

It appears from the above that a model for superplasticity must explain and predict the following:

(1) the strain-rate is proportional to $(\frac{\tau}{d})^2$;

(2) the activation energy for deformation is equal to that for grain-boundary diffusion;

(3) the constant A has a value of $\sim$200;

(4) there is no dislocation activity in the interior of the grains.[21]

Region III: As noted earlier there is no apparent grain-size dependence of the strain-rate in this region and the activation energy for creep is about 1.7 times that observed in regions I and II. Experimental results in this stress range indicate stress exponents of the order of 4. Such a τ^4 dependence in addition to the approximate equivalence of the activation energy for flow in this region and that for self-diffusion suggest a dislocation model such as climb[8] of edge dislocations. The experimental value for A of $(1.34 \pm 1.03) \times 10^6$ supports such a contention. The experimental data on high temperature creep in pure aluminum yields a value of 6×10^7 for A when climb model is applicable.[4] It thus

appears that climb of dislocations controls the deformation in this region.

To summarize the above observations $\ln \frac{\dot{\gamma}kT}{D_b Gb}$ was plotted versus $\ln \frac{\tau}{G}$ in Fig. 9 for two grain sizes (1.2 and 4.6 μm). The experimental results are shown by datum points connected by dashed lines. To compare the experimental results with various theories, the theoretical curves expected from Nabarro-Herring,[9,10] Coble,[11] superplastic (Ball-Hutchison model)[5], dislocation climb[4,8] as well as viscous glide[4,16] mechanisms are also plotted in Fig. 9. Also included herein are the theoretical lines predicted by the Nabarro-Herring mechanism in sub-grains[16] as well as the Nabarro-Bardeen-Herring[24] mechanism based on the climb of dislocations from Bardeen-Herring sources. Table I summarizes the parameters obtained through the various diffusion-controlled creep models along with those found in the various regions in the present work. It is clear from Fig. 9 that Coble, Superplastic and Climb mechanisms operate in the regions I, II and III respectively. In addition the contribution to the deformation-rates in Zn-22 Al of the other mechanisms which may simultaneously be operating is negligible in the stress range from $5 \times 10^{-7}G$ to $5 \times 10^{-3}G$.

ACKNOWLEDGMENTS

This work was supported by the United States Atomic Energy Commission through the Inorganic Materials Research Division of the Lawrence Berkeley Laboratory of the University of California, Berkeley. One of the authors (KLM) is thankful to Professor J. W. Morris, Jr. for his interest in the present work and for a critical reading of the manuscript. MLV wishes to acknowledge the Kanpur-Indo-American Programme under USAID for financial support

REFERENCES

1. E. E. Underwood, J. Metals, 14, 914 (1962).

2. R. H. Johnson, Metal Mater., 4, 115 (1970).

3. G. J. Davies, J. W. Edington, C. P. Cutler and K. A. Padmanabhan, J. Mat. Science 5, 1091 (1971).

4. J. E. Bird, A. K. Mukherjee and J. E. Dorn, "Quantitative Relation Between Properties and Microstructure," D. G. Brandon and A. Rosen (eds.), Israel University Press, Haifa (1969).

5. A. Ball and M. M. Hutchison, Matal Sci. J., 3, 1 (1969).

6. E. W. Hart, Acta Met., 15, 1545 (1967).

7. D. H. Avery and W. A. Backofen, Trans. ASM, 58, 551 (1965).

8. J. Weertman, J. Appl. Phys. 26, 1213 (1955).

9. F.R.N. Nabarro, "Rept. of Conf. on the Strength of Solids," The Physical Society, London (1948) p. 75.

10. C. Herring, J. Appl. Phys. 21, 437 (1950).

11. R. L. Coble, J. Appl. Phys. 34, 1679 (1963).

12. C. M. Packer and O. D. Sherby, Trans. ASM, 60, 21 (1967).

13. R. C. Gifkins, J. Inst. Metals, 95, 373 (1967).

14. R. C. Gifkins, J. Amer. Ceramic Soc., 51, 69 (1968).

15. R. R. Vandervroot, A. K. Mukherjee and J. E. Dorn, Trans. ASM, 59, 930 (1966).

16. K. Linga Murty, F. A. Mohamed and J. E. Dorn, LBL Report #442, (1971), to be published.

17. D. M. Schwartz, J. B. Mitchell and J. E. Dorn, Acta Met., 15, 485 (1967).

18. J. J. Spokas and C. P. Slichter, Phys. Rev. 113, 1462 (1969); also T. S. Lundy and J. F. Murdock, J. Appl. Phys. 33, 1671 (1962).

19. E. S. Wajda, Acta Met., 2, 184 (1954).

20. A. Hassner, Isotopenpraxis, 5, 148 (1969).

21. R. B. Nicholson, in the International Materials Symposium, University of California, Berkeley (1971).

22. T. G. Langdon, Phil. Mag. 22, 689 (1970).

23. D. J. Dingley, Scanning Electron Microscopy Conference, Chicago, (1970) p. 329.

24. F.R.N. Nabarro, Phil. Mag. 16, 231 (1967).

TABLE I

Creep parameters α, m, n and A in the emperical equation

$$\frac{\dot{\gamma}kT}{D_b Gb} = A\left(\frac{b}{d}\right)^m \left(\frac{\tau}{G}\right)^n \left(\frac{D}{D_b}\right)^\alpha \quad ,$$

obtained in the present experiments and those predicted by various diffusional creep theories.

Mechanism	α	m	n	A	Reference
Region I	0	3	1	55 ± 25	Present Study on Zn-22 Al
Region II	0	2	2	302 ± 216	
Region III	1	0	4	$(1.34 \pm 1.03) \times 10^6$	
Nabarro-Herring	1	2	1	12	Nabarro[9], Herring[10]
Coble	0	3	1	100	Coble[11]
Superplastic	0	2	2	200	Ball and Hutchison[5]
Climb (Al)	1	0	4	6×10^7	Bird, Mukherjee and Dorn[4]; Weertman[8]
Glide	1	0	3	6	Bird, Mukherjee and Dorn[4]
Nabarro-Subgrain	1	0*	3	0.12	Murty, Mohamed and Dorn[16]
	1	2†	1	12	
Nabarro-Bardeen-Herring	1	0	3	$1/\pi(\ln 4G/\pi\tau)$	Nabarro[24]
	0§	0	5	7.4×10^{-2}	

* With $\frac{b}{\delta} = 0.1\ (\tau/G)$, here δ = mean subgrain diameter.

† With d = δ = mean subgrain diameter, here δ is independent of the applies stress.[16]

§ Assuming $D_c = D_b$, here D_c = dislocation core diffusivity

FIGURE CAPTIONS

1. Predicted trends of deformation mechanisms in a superplastic material. Comparison of mechanisms controlled by Coble, Superplastic and dislocation Climb creep at low, intermediate and high stress regions.[4]

2. Drawing of the double-shear type test specimens.

3. Double-log plot of the steady-state shear strain-rate versus the applied shear stress at 250°C.

4. Dependence of the strain-rate on the grain size. Double-log plots indicate d^{-3} and d^{-2} dependencies of the creep-rate respectively in the regions I and II.

5a. Arrhenius plot of the logarithm of the strain-rate versus 1/T in the region I.

5b. The temperature dependence of the steady-state strain-rate in the region II plotted as $\ln \dot{\gamma}\, GT$ versus 1/T.

5c. Arrhenius plot of the temperature compensated strain-rate plotted as $\ln \dot{\gamma}\, G^3\, T$ versus 1/T in the region III.

6. Plot of '$\ln \frac{\dot{\gamma} kT}{D_b Gb}$ vs $\ln \frac{\tau}{G}$' depicting the grain size dependence. In the regions I and II, datum points obtained at various temperatures for the four grain sizes were shown while in the region III, the data obtained at different temperatures for only the largest grain-size were plotted for simplicity.

7. Plot of '$\ln \frac{\dot{\gamma} kT}{D_b Gb}$ vs $\ln \frac{\tau}{G}$' for two grain size values, d = 4.6 μm and d = 3.6 μm at various temperatures showing the transition from region II to region III. Theoretical predictions based on the dislocation climb model for the different temperatures were shown in the region III for comparison with the experimental results.

8. Data of Nuttall taken from reference 21 plotted as '$\ln \frac{\dot{\gamma} kT}{D_b Gb}$ versus $\ln \frac{\tau}{G}$' to show that n is <u>not</u> a continuous function of temperature in the 'Superplastic' region. As is clear from this plot, the data at various temperatures coalesced into a single line in the stress range $\sim 5 \times 10^{-6}$ G to $\sim 10^{-4}$G and start deviating into separate lines as the 'climb' region is approached at higher stresses.

9. Comparison of the experimental results obtained for the two grain-size values, 1.2 μm and 4.6 μm, with the theoretical lines obtained from various creep models.

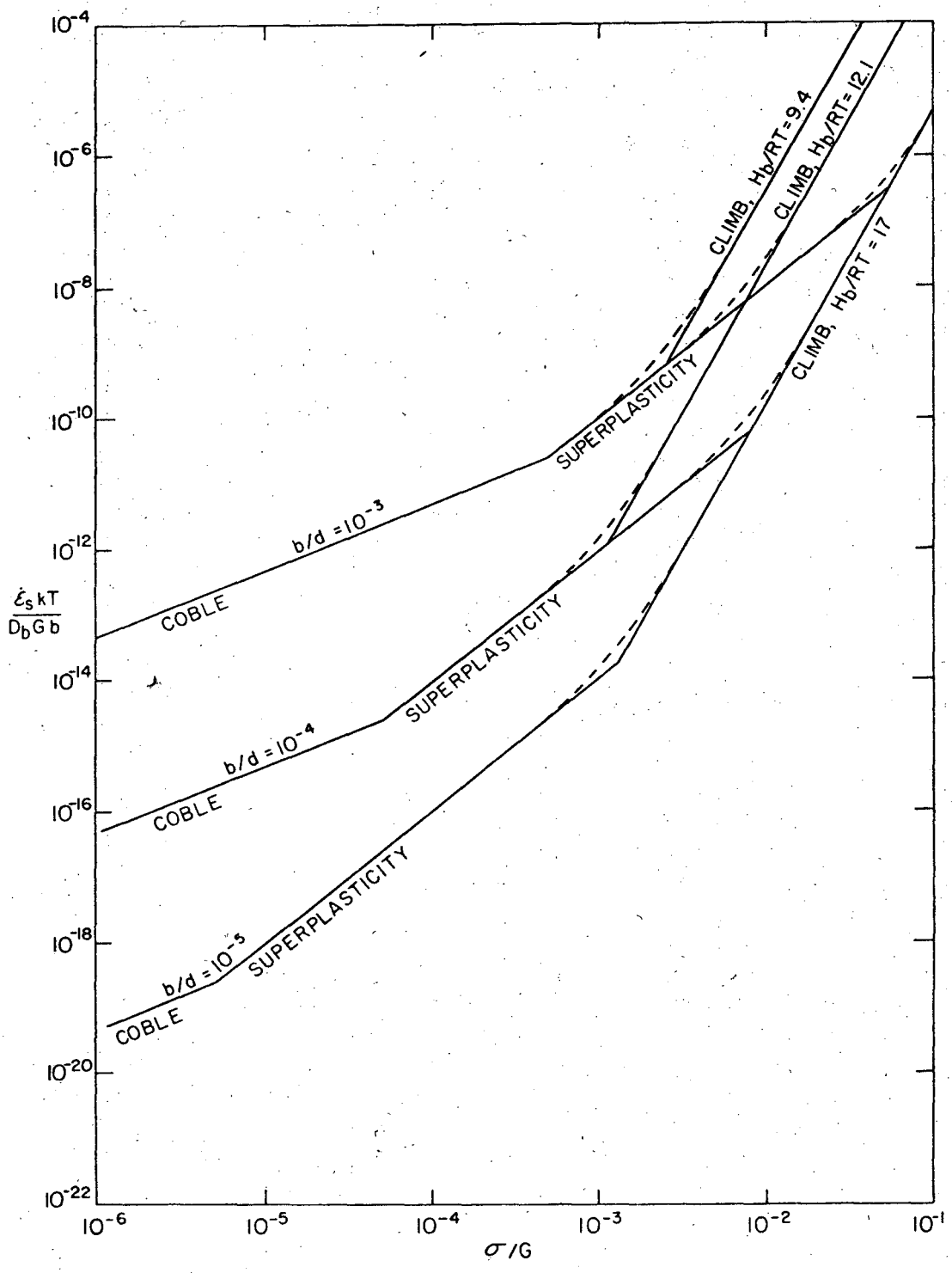

XBL 697-1044

Fig. 1

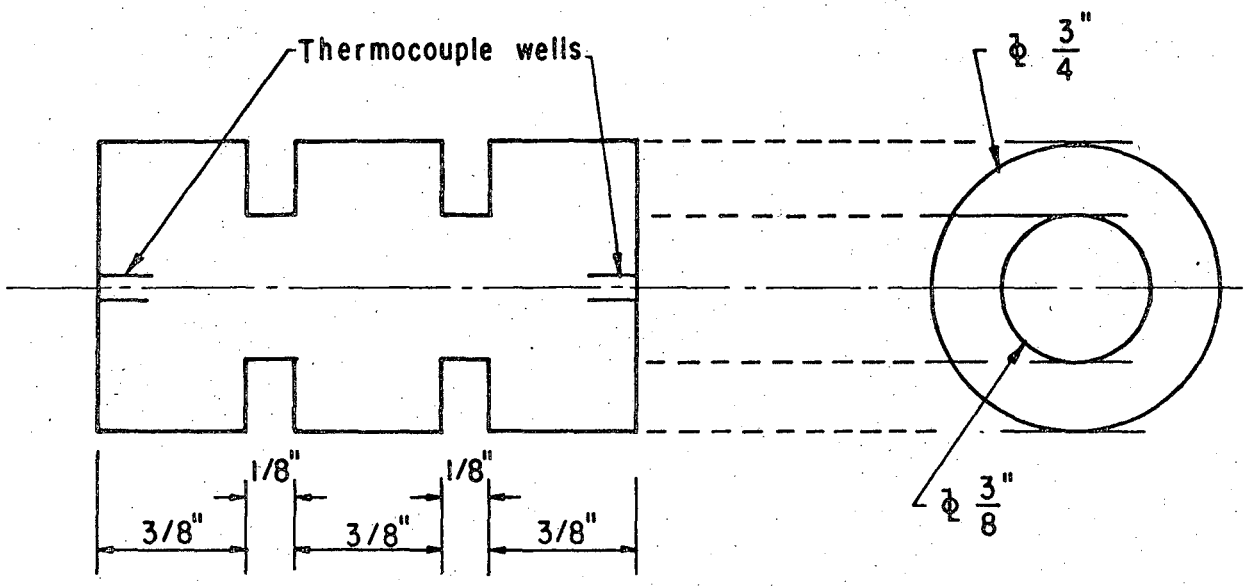

XBL 721-5935

Fig. 2

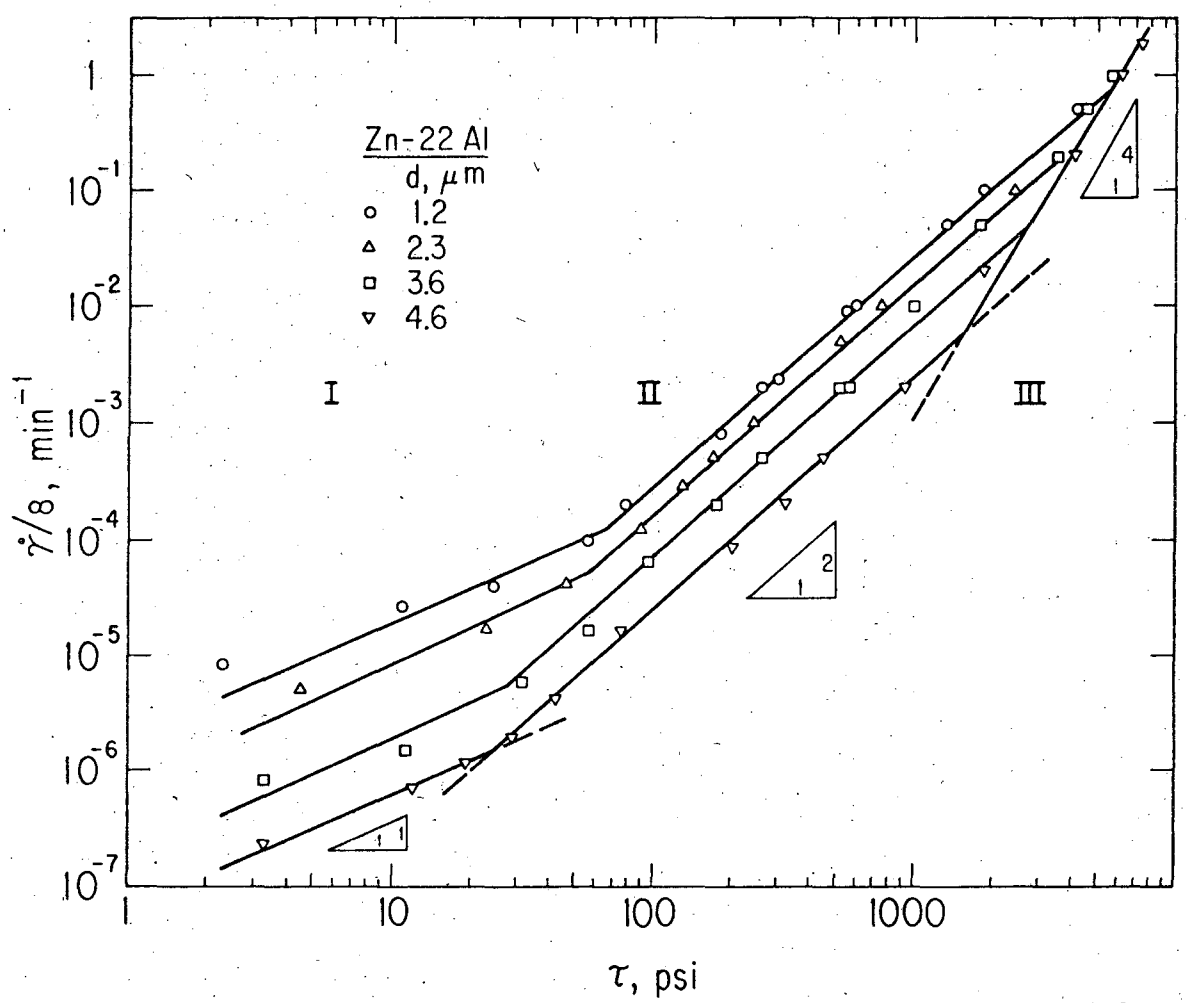
Zn-22 Al
d, μm
1.2
2.3
3.6
4.6
I
II
III
4
1
2
1
1
1
10^-1
10^-2
10^-3
10^-4
10^-5
10^-6
10^-7
1
10
100
1000
γ̇/8, min^-1
τ, psi
XBL 721-5936

Fig. 3

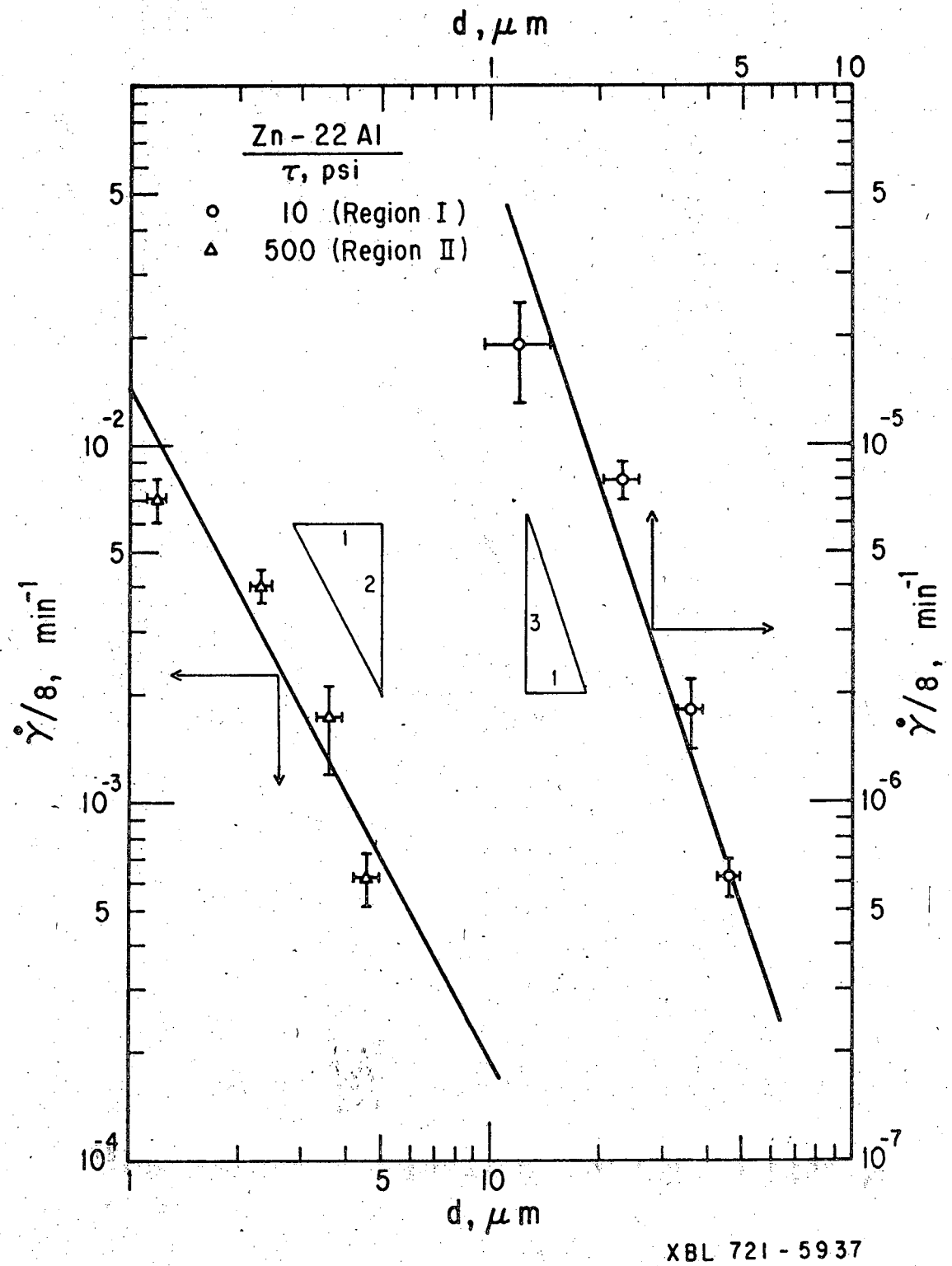
d, μm
Zn - 22 Al
τ, psi
10 (Region I)
500 (Region II)
1
2
3
1
γ̇/8, min⁻¹
γ̇/8, min⁻¹
d, μm
XBL 721 - 5937

Fig. 4

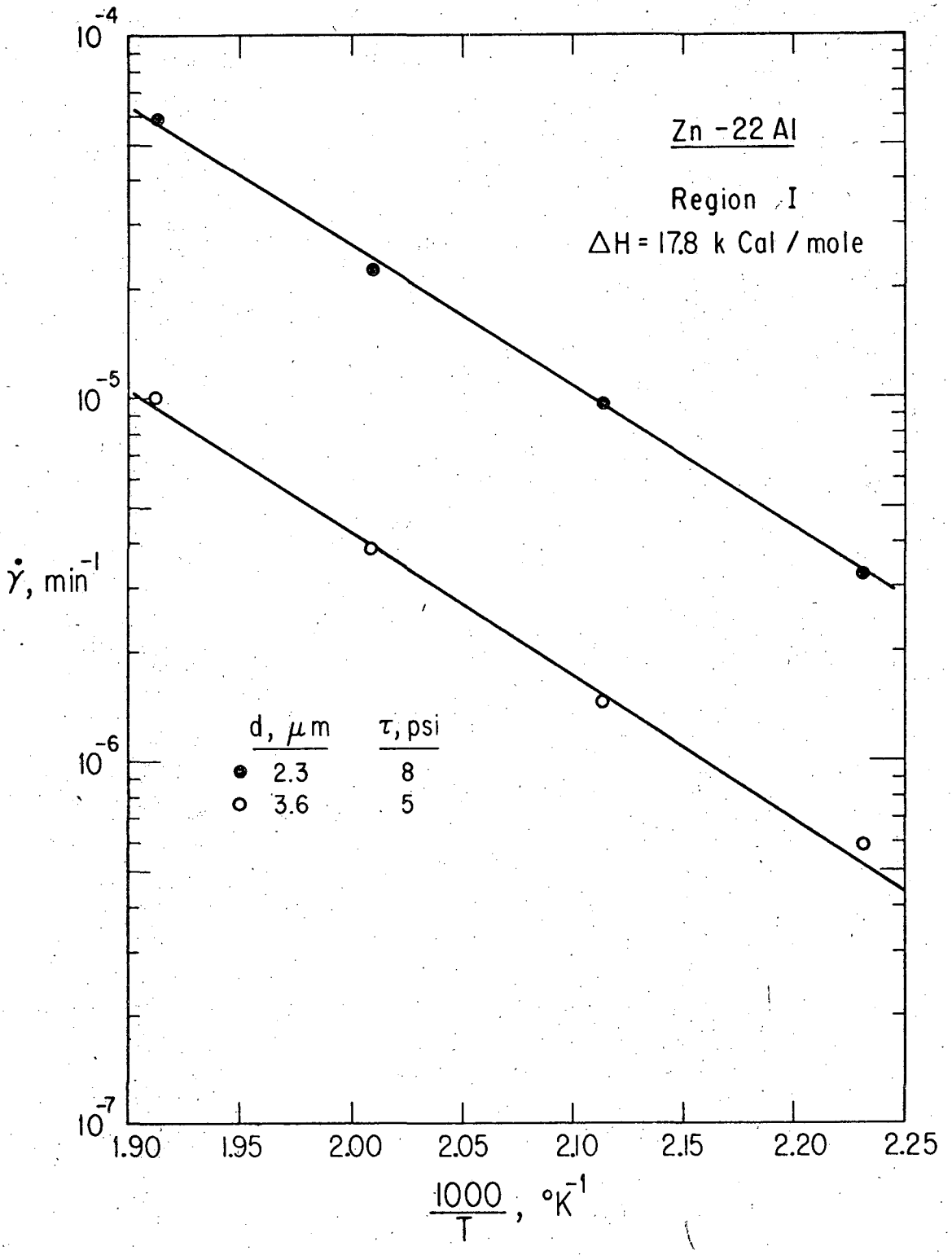
Zn -22 Al
Region I
ΔH = 17.8 k Cal / mole
d, μm
τ, psi
2.3
8
3.6
5
$\dot{\gamma}$, min^{-1}
10^{-4}
10^{-5}
10^{-6}
10^{-7}
1.90
1.95
2.00
2.05
2.10
2.15
2.20
2.25
$\frac{1000}{T}$, °K^{-1}
XBL 721-5938

Fig. 5

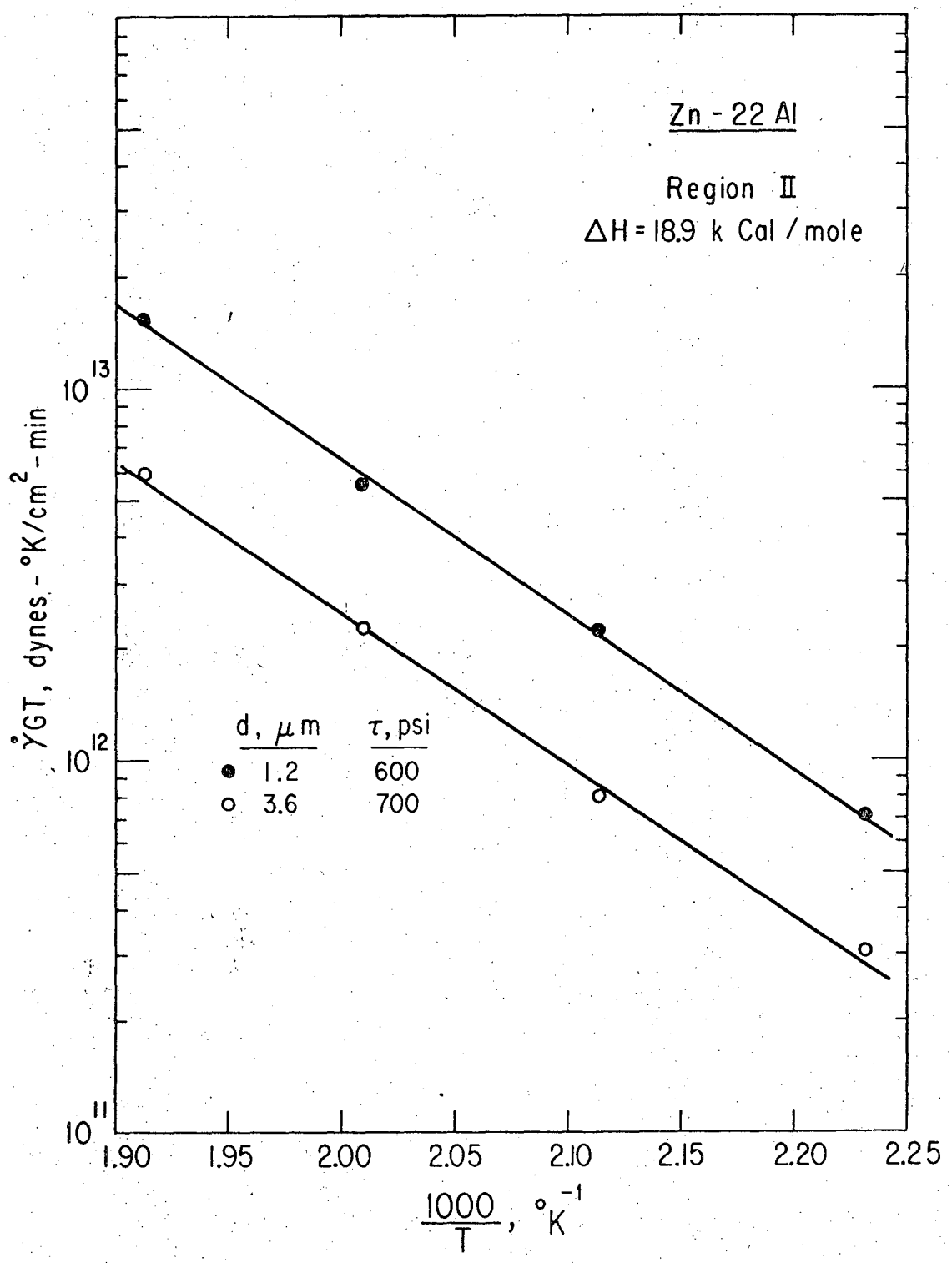
Zn - 22 Al
Region II
ΔH = 18.9 k Cal / mole
d, μm
τ, psi
1.2
600
3.6
700
$\dot{\gamma}_{GT}$, dynes - °K/cm² - min
10^{13}
10^{12}
10^{11}
1.90
1.95
2.00
2.05
2.10
2.15
2.20
2.25
1000/T, °K⁻¹
XBL 721-5939

Fig. 6

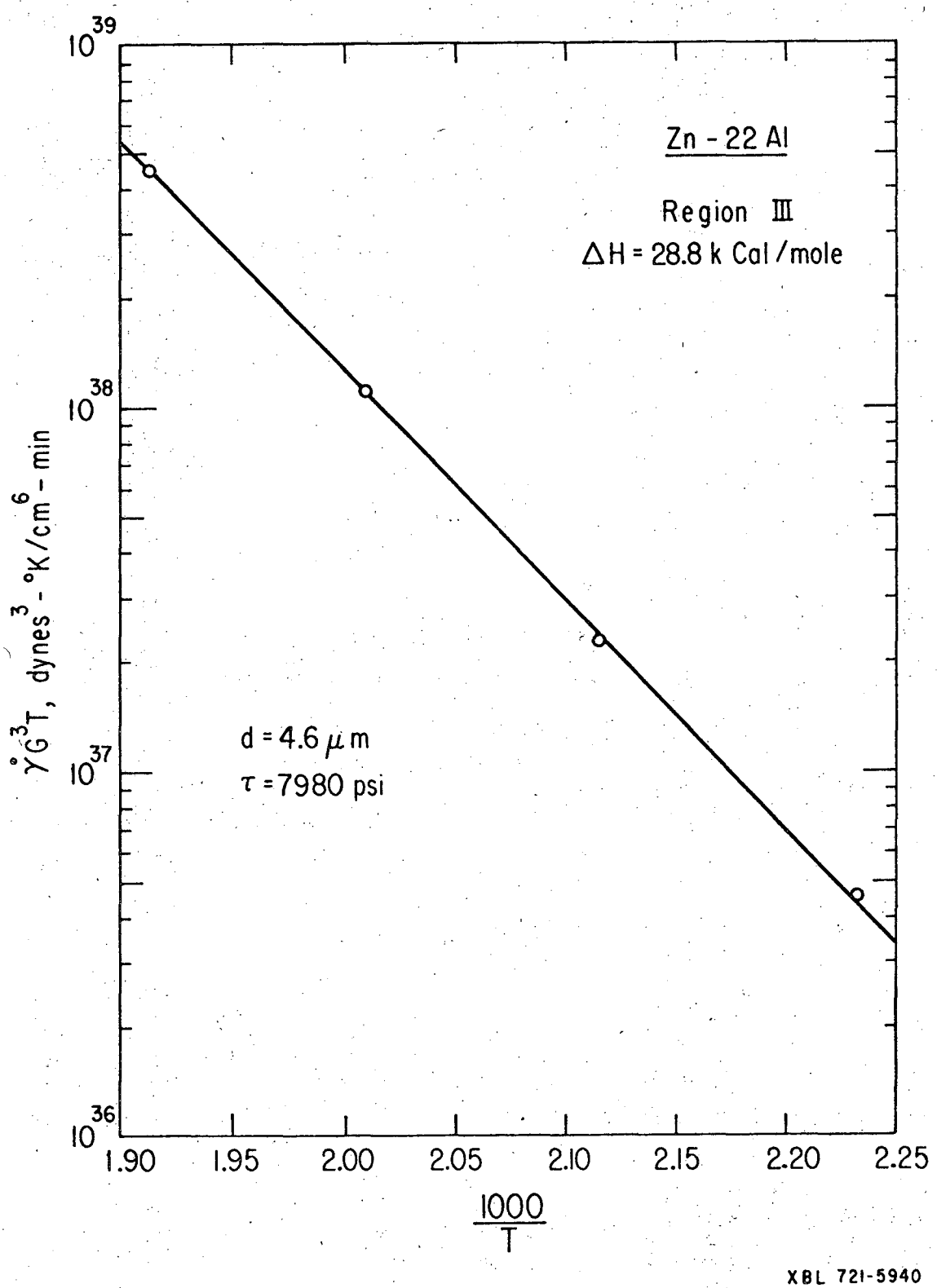
Zn - 22 Al
Region III
ΔH = 28.8 k Cal / mole
d = 4.6 μm
τ = 7980 psi
$\dot{\gamma} G^3 T$, dynes^3 - °K/cm^6 - min
10^{39}
10^{38}
10^{37}
10^{36}
1.90
1.95
2.00
2.05
2.10
2.15
2.20
2.25
$\frac{1000}{T}$
XBL 721-5940

Fig. 7

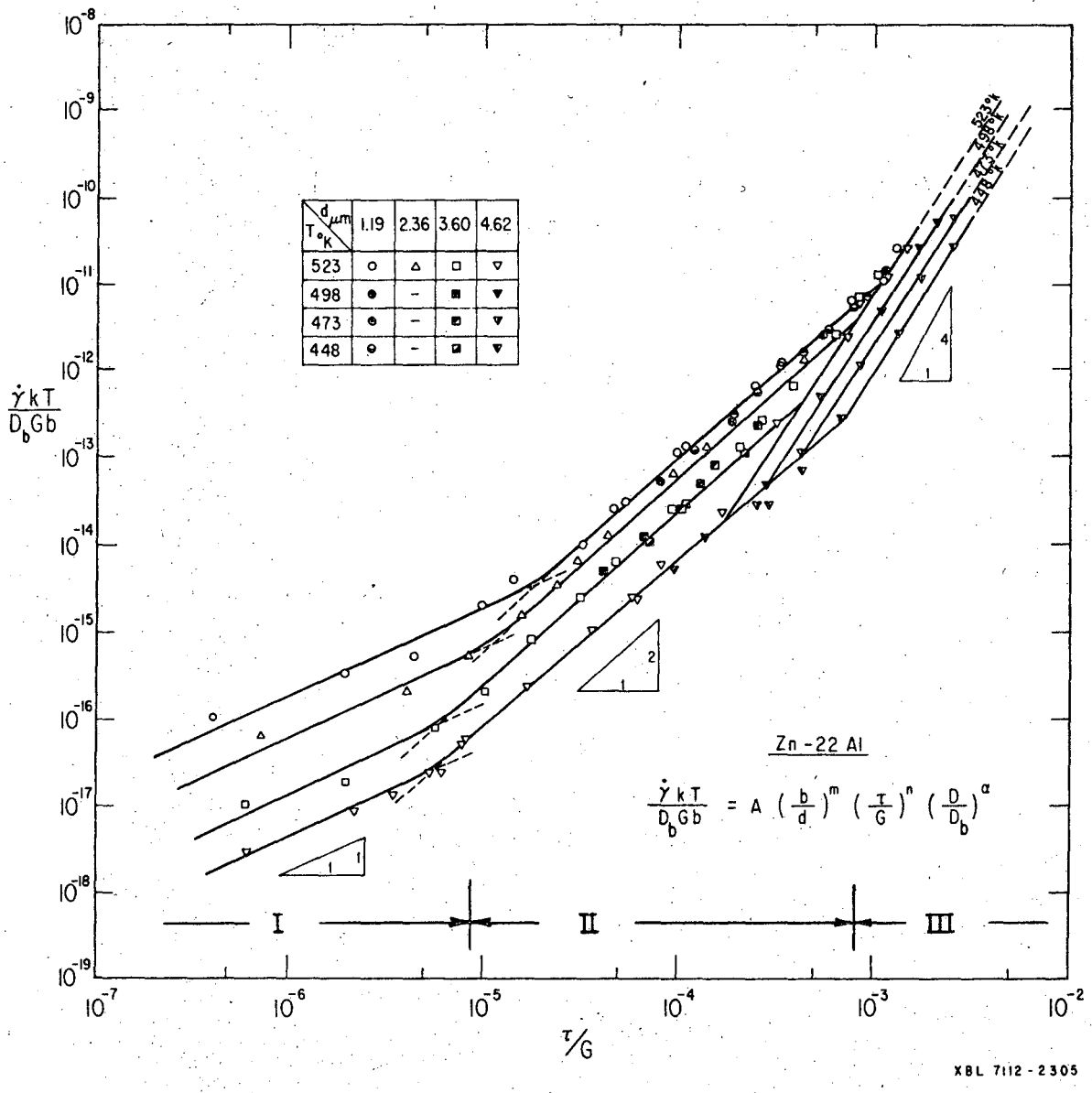
$\frac{\dot{\gamma} k T}{D_b G b}$
τ/G
10^{-8}
10^{-9}
10^{-10}
10^{-11}
10^{-12}
10^{-13}
10^{-14}
10^{-15}
10^{-16}
10^{-17}
10^{-18}
10^{-19}
10^{-7}
10^{-6}
10^{-5}
10^{-4}
10^{-3}
10^{-2}
d μm
T °K
1.19
2.36
3.60
4.62
523
498
473
448
523°K
498°K
473°K
448°K
4
1
2
1
1
1
Zn - 22 Al
$\frac{\dot{\gamma} k T}{D_b G b} = A \left(\frac{b}{d}\right)^m \left(\frac{\tau}{G}\right)^n \left(\frac{D}{D_b}\right)^\alpha$
I
II
III
XBL 7112 - 2305

Fig. 8

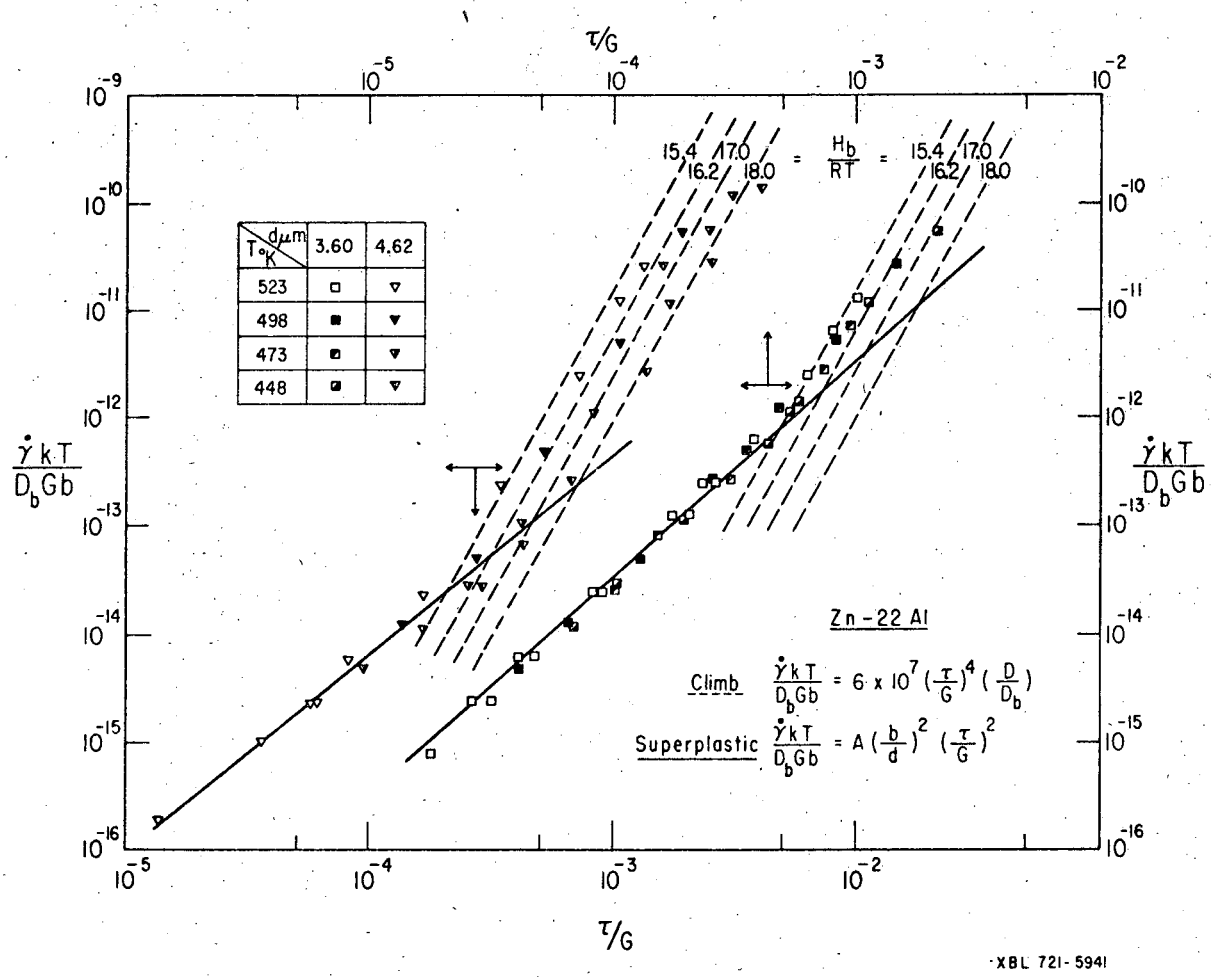
τ/G
10^{-5}
10^{-4}
10^{-3}
10^{-2}
10^{-9}
10^{-10}
10^{-11}
10^{-12}
10^{-13}
10^{-14}
10^{-15}
10^{-16}
15.4 17.0 16.2 18.0 = $\frac{H_b}{RT}$ = 15.4 17.0 16.2 18.0
$T_{°K}$ \ d μm | 3.60 | 4.62
523 | □ | ▽
498 | ■ | ▼
473 | ▣ | ▼
448 | ▣ | ▽
$\frac{\dot{\gamma} k T}{D_b G b}$
Zn - 22 Al
Climb $\frac{\dot{\gamma} k T}{D_b G b} = 6 \times 10^7 (\frac{\tau}{G})^4 (\frac{D}{D_b})$
Superplastic $\frac{\dot{\gamma} k T}{D_b G b} = A (\frac{b}{d})^2 (\frac{\tau}{G})^2$
XBL 721-5941

Fig. 9

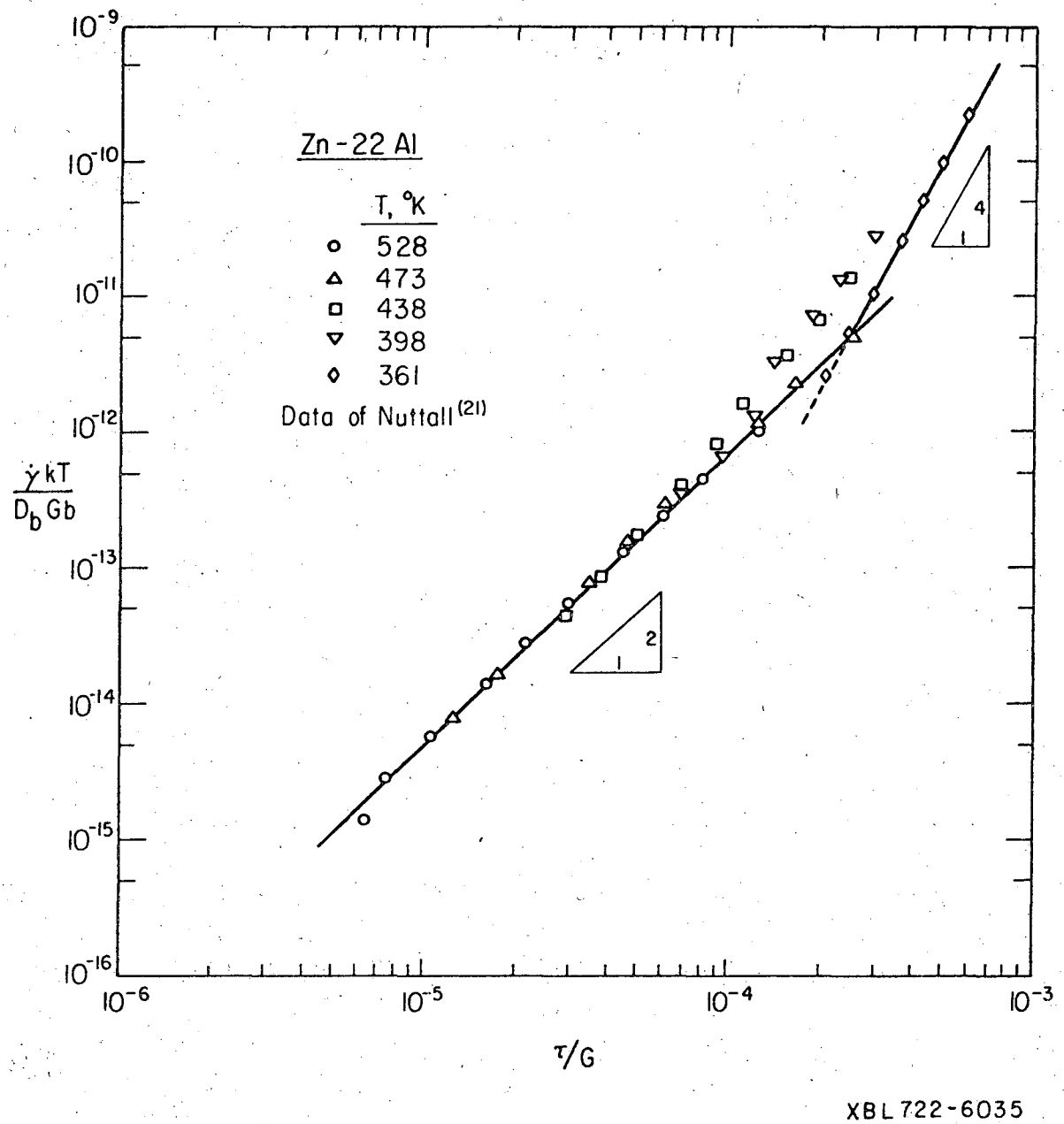
Zn - 22 Al
T, °K
528
473
438
398
361
Data of Nuttall(21)
4
1
2
1
$\frac{\dot{\gamma} kT}{D_b Gb}$
τ/G
10^{-9}
10^{-10}
10^{-11}
10^{-12}
10^{-13}
10^{-14}
10^{-15}
10^{-16}
10^{-6}
10^{-5}
10^{-4}
10^{-3}
XBL 722-6035

Fig. 10

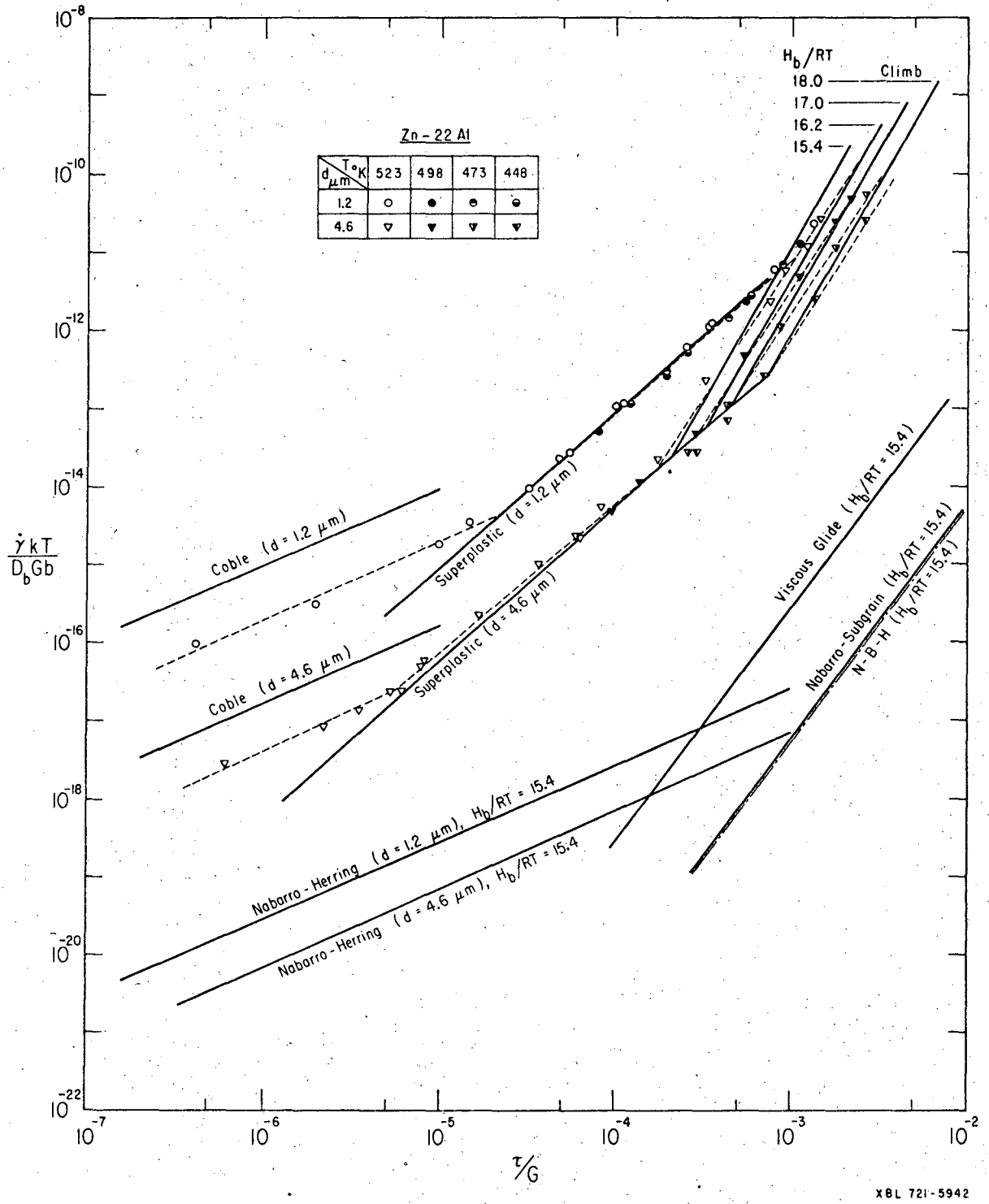
Zn - 22 Al
d μm \ T°K | 523 | 498 | 473 | 448
1.2
4.6
H_b/RT
18.0 Climb
17.0
16.2
15.4
Coble (d = 1.2 μm)
Superplastic (d = 1.2 μm)
Coble (d = 4.6 μm)
Superplastic (d = 4.6 μm)
Viscous Glide (H_b/RT = 15.4)
Nabarro-Subgrain (H_b/RT = 15.4)
N-B-H (H_b/RT = 15.4)
Nabarro-Herring (d = 1.2 μm), H_b/RT = 15.4
Nabarro-Herring (d = 4.6 μm), H_b/RT = 15.4
$\frac{\dot{\gamma} kT}{D_b Gb}$
τ/G
10^{-8}
10^{-10}
10^{-12}
10^{-14}
10^{-16}
10^{-18}
10^{-20}
10^{-22}
10^{-7}
10^{-6}
10^{-5}
10^{-4}
10^{-3}
10^{-2}
XBL 721-5942

Fig. 11

TECHNICAL INFORMATION DIVISION
LAWRENCE BERKELEY LABORATORY
UNIVERSITY OF CALIFORNIA
BERKELEY, CALIFORNIA 94720